

COUPLED HYDRO-MECHANICAL MODELLING OF THE GPK3 RESERVOIR STIMULATION AT THE EUROPEAN EGS SITE SOULTZ-SOUS-FORÊTS

T. Kohl and T. Mégel

GEOWATT AG
Dohlenweg 28
CH-8050 Zürich; Switzerland
e-mail: kohl@geowatt.ch

ABSTRACT

In 2004 the European EGS project got into its decisive state when reaching the targeted reservoir depth. Currently, three boreholes, (GPK2, GPK3 and GPK4) have been drilled to 5 km. Improvement of the reservoir conditions by stimulation and minimizing the seismic risk represents now a primary challenge to enable economic operation and future extension. In this context, the new HEX-S code has been developed to simulate the transient hydro-mechanical response of the rock matrix to massive hydraulic injections. The present paper describes the modeling results of the GPK3 stimulation starting at May 27, 2003. Maximum flow rates of >60 l/s have been used, triggering >30'000 microseismic events. The transient numerical simulation intends to obtain a match of both, the microseismic and the hydraulic behavior. Different model calculations demonstrate the capabilities of our new approach. It is noteworthy that the modeling became possible only due to the excellent data quality at the Soultz project. The results demonstrate that simulations based on solid physical ground can reveal the complex reservoir behavior during hydraulic stimulation. The use of HEX-S also provides perspectives for future developments such as design calculations that enable optimizing cost-intensive hydraulic stimulations before hand.

INTRODUCTION

In 2004, the final borehole of the current pilot phase at the European EGS site Soultz-sous-Forêts (France) has been drilled. Details of the project are described by e.g. Baria et al. (2000). The planned triplet consists of the two boreholes GPK2 and GPK4 as producers and a central borehole, GPK3 as injector. The boreholes are aligned in roughly N-S direction, reflecting the normal/strike-slip stress regime at the Rhine-Graben location. Recently, the 5 km reservoir

has been stimulated by three major injections at each borehole during 2002 – 2004. Details of the current measurement program is described in Gérard (2004)

Since the fracture at GPK2 could only be roughly estimated (see later), the present paper is concentrating on the GPK3 injection test from May 27th to June 06th, 2003. Flow rate has been varied at several steps up to > 60 l/s at short term and more than 30'000 microseismic events have been recorded. Fig.1 illustrates the seismic response to the change in flow rate: clearly, each flow step change is accompanied by a variation of seismicity, with increasing seismicity at increasing hydraulic flow rate.

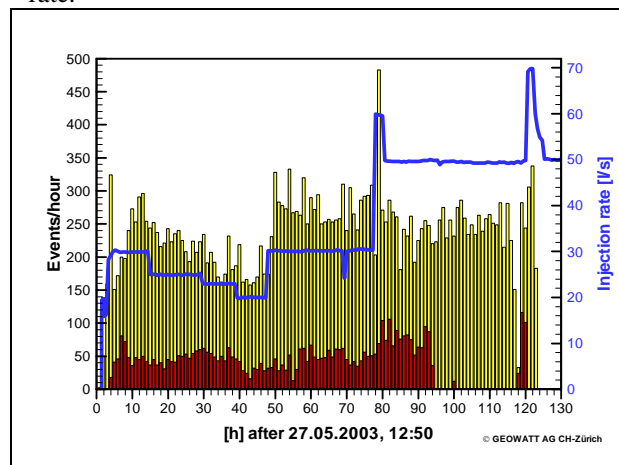


Fig. 1. Flow rate (right axis) and induced seismicity (left axis) during the 2003 stimulation of GPK3. The located seismic events – normalized on 1 hr intervals - represent only a fraction of the total number and are illustrated by a darker colour.

The connection between hydraulic and brittle elastic processes is obvious and has also been observed at various other circumstances and locations. This evidence led us to the development of the new code HEX-S. It was envisaged to model the hydraulic and

seismic processes in a way that the complex non-linear processes are characterized on solid physical ground. Especially, the code should reproduce the observed transient 3-D evolution of shear events in the rock matrix in space and time, as well as the downhole pressure observed in the boreholes.

STIMULATION OF GPK3

The hydro-mechanical code HEX-S

The hydro-mechanical code HEX-S has been developed to calculate the stimulation processes in a fractured reservoir during a massive injection into a borehole. The code takes into account the aperture change of each fracture in the model due to the corresponding overpressure resulting from the injection. The propagation of the overpressure in the reservoir as well as the development of the highly anisotropic reservoir permeability as a result of the fracture apertures is calculated as a time-dependent process.

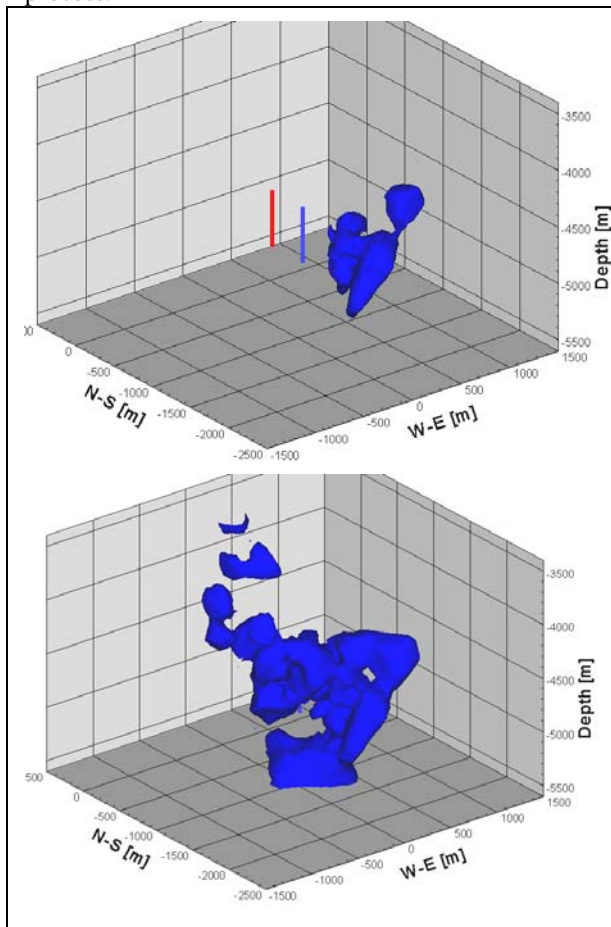


Fig. 2.: Calculated iso-surface of the 0.1 mm fracture aperture after 5 hours (top) and 20 hours (bottom) of injection into GPK4 for the 5 km deep reservoir domain at Soutz-sous-Forêts

Hence the reaction of the reservoir permeability due to an arbitrary injection rate history can be calculated. Fig. 2 illustrates the typical transient development of a 0.1 mm aperture change in a fractured reservoir due to hydraulic injection..

Generation of the fracture network

The permeability distribution in a HEX-S model depends essentially on the location, orientation and aperture of the incorporated fractures. HEX-S allows defining an arbitrary number of both, stochastic and deterministic, fracture sets. Experience from various EGS test sites demonstrates that microseismic events often follow planar structures (i.e. Asanuma 2004, Evans et al. 2005; Cuenot et al. 2005). Since we assume that in most cases an induced microseismic event represents the shear failure of a along an area of a fracture ("slip patch"), the locations of the calculated shearing events can be compared with the microseismic clouds. In contrary, possible mode I events (normal stress variations) remain unidentified. In HEX-S every fracture or fracture zone is represented by a number of circular slip patches with small, predefined radii, generated by subdivision of a planar, and so far circular fracture zone. The aperture of each specific slip patch contributes to the final permeability distribution in the model. Starting from an initial value (see below), the aperture change of a fracture depends on the orientation, the local effective stress field and its defined mechanical parameters.

Each fracture zone in HEX-S can be generated from deterministic or stochastic data, with the following detailed properties:

1. Deterministic fracture zones of defined radii, orientations and classes of mechanical behaviour for their slip patches: The corresponding data is generally derived from borehole logs (e.g. FMS, UBI) but may also include post-experimental interpretation of individual, microseismically active planar structures (Fig. 3).
2. Stochastic generation of fracture zones with random location and orientation: The statistical distribution of the orientation of fracture zones seen in borehole logs is used as the input parameter for the stochastic generation. Each random seed number generates a new distribution of fracture zones in the model (Fig. 4). Each stochastically generated model, independent from the random seed number, has the same distribution of orientations of fracture zones. Stochastically generated fracture zones are generally reasonably used at locations with little information (i.e. at greater distance from the boreholes). The herewith-defined model domain is filled-up until a predefined fracture (or slip

patch) density is reached. Generally, sets of >20'000 slip patches are generated in this way.

The initial aperture of each slip patch is proportional to its radius and adjusted with an overall factor in such a way that the whole reservoir model has a predefined average permeability.

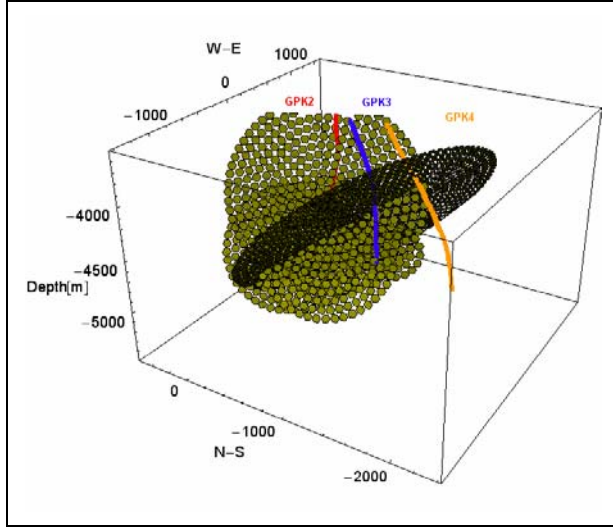


Fig. 3: Example of a model with deterministic fracture zones subdivided into slip patches for the 5 km deep reservoir domain at Soutz-sous-Forêts. Also indicated are the boreholes GPK2, GPK and GPK4

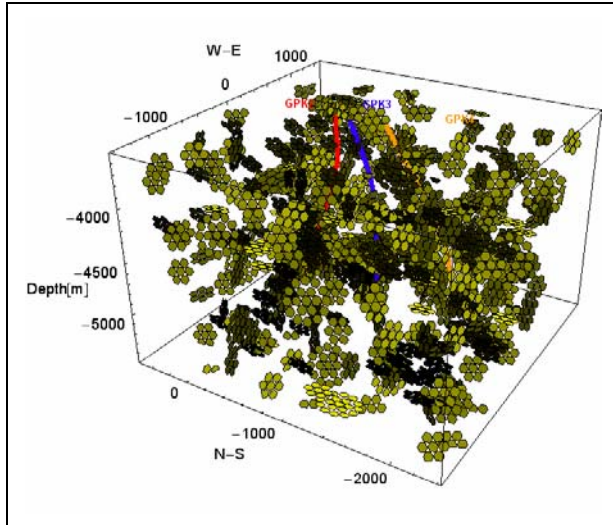


Fig. 4: Example of stochastically generated fracture zones for the 5 km deep reservoir domain at Soutz-sous-Forêts. Also indicated are the boreholes GPK2, GPK and GPK4

Implemented fracture aperture laws

The implemented aperture laws for the fractures or slip patches are basically of analytical kind (Willis-

Richards et al., 1996, Jing et al., 1998, Bächler et al., 2001). The aperture of a fracture depends on three sets of parameters:

1. The mechanical properties of the fracture
2. The fluid pressure in the fracture space
3. The normal and the shear stress on the fracture plane

The effective normal stress $\sigma_{n,eff}$ and the effective shear stress τ_{eff} on the plane of a fracture are derived from the three regional principal stress components and the fluid pressure P at the fracture location. Depending on the pore and fracture fluid pressure P , the fracture aperture at a given location is assumed to react:

- a) By compliance only
- b) By compliance and shearing
- c) By jacking and shearing

a. Compliance only

Under the condition of low effective shear stress, τ_{eff} , only a compliant reaction of the fracture walls to fluid pressure will affect the aperture. The conditions for this behaviour are

$$\sigma_{n,eff} > 0$$

$$\Delta\tau = \tau_{eff} - \sigma_{n,eff} \cdot \tan(\Phi) < 0$$

(Mohr-Coulomb criterion)

As convention, stress is positive for compression. The friction angle Φ of the fracture walls is implemented as a function of $\sigma_{n,eff}$. The aperture increase is treated as reversible and vanishes as soon the pressure declines after the end of injection.

b. Compliance and shearing

If the effective shear stress τ_{eff} at the fracture walls exceeds the friction resistance, i.e. $\Delta\tau > 0$, and the effective normal stress $\sigma_{n,eff}$ still is positive, the fracture fails. The additional "shear" aperture change, a_s , due to the shear offset, U , is

$$a_s = U \cdot \tan(\Phi_{dil})$$

The shear dilation angle of the fracture wall, Φ_{dil} , is also implemented as function of $\sigma_{n,eff}$. The shear offset is defined from fracture shear stiffness, K_s , as:

$$U = \Delta\tau / K_s$$

This portion of the aperture increase is considered to be irreversible when injection test has stopped and the pressure field in the reservoir has reached its ambient value.

c. Jacking and shearing

In the case the effective normal stress, $\sigma_{n,eff}$, becomes negative, the fracture walls separate and the friction forces acting on them disappear. In addition to the shear aperture change, a contribution from jacking conditions, a_j , arises. Clearly, a_j is considered to be fully reversible.

Although the shear induced, mode II, aperture change of a fracture is the only permanent effect after an injection test has ended, the contributions from jacking and compliance are also of major importance for the propagation of the pressure front during the stimulation process.

Hydraulic processes

The time-dependent pressure calculation in HEX-S is performed with a new finite element (FE) algorithm which is a further development of the FRACTure code (Kohl & Hopkirk, 1995). The main advantages of the FE algorithm are in efficient and flexible formulations:

- Local mesh refinement at specified locations in the reservoir domain such as boreholes,
- Utilization of an implicit time-step procedure for the transient calculation
- Easy extension to further physical processes or constitutive laws

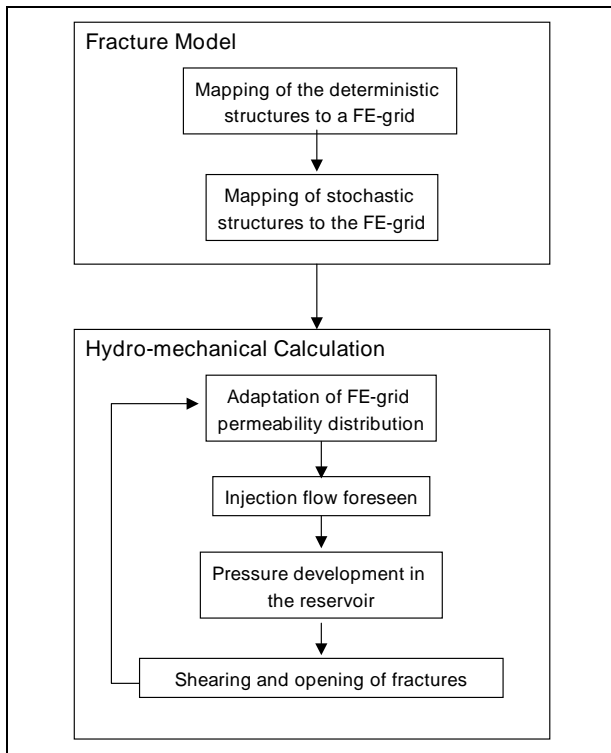


Fig. 5: Principle flow chart of HEX-S

The hydraulic conductivity for each element is derived from the apertures of the intersecting slip patches by a specific mapping procedure. The intersection of the discrete fractures with the continuous FE grid is calculated using a "Rock-to-Fracture volumetric index", RFVI. The mapping results in individual FE volumes of strongly anisotropic properties. Thereby, the hydraulic properties of the FE grid are modified after each time-step. HEX-S calculates the pressure in the model and determines the new apertures of the slip patches. When the hydraulic conductivities of the elements have been updated from the corresponding slip patch apertures, a next time-step is carried out (Fig. 5).

Model of GPK2/GPK3

The numerical model used for the simulation of the hydraulically induced shearing events consists of ~450'000 nodes, covering a surface area of 12x10 km² and a total depth range of 3000-6000 m. As general Soultz convention, the origin of the model (coordinates 0/0/0) is set to the head of the 3.5 km deep GPK1 borehole. The model is strongly refined towards its center, along the stimulated open-hole sections of GPK2, GPK3 and GPK4 between 4500-5000m depth. Fig. 6 illustrates this refinement in vertical and horizontal direction. Towards the boreholes, hexahedrons with partly less than 25x25x25m³ have been applied. The hydraulic behavior along the open-hole sections of the boreholes is simulated using vertical 1D elements. The hydraulic boundary conditions account for the large vertical fault zones in the Rhine Graben area. Hence, Dirichlet boundary conditions ($\Delta P=0$) best describe such drainage systems along the lateral borders. The injected flow is simulated as Neuman boundary condition at the top of the open-hole section (i.e. at the topmost part of the 1-D borehole element). GPK2 was shut-in during the first stimulation phase. The variation of flow rate is controlled in the model by load-time functions that allow specifying the transient change of boundary conditions at arbitrary time intervals.

In a preliminary compilation of R. Maurer (2004), a total of 17 deterministic fractures for GPK2 and GPK3 were implemented into the stimulation model. Location of the GPK2 hydraulically active fractures, which permit the fluid circulation between the reservoir and the borehole, had to be determined by the BRGM (French Geological Survey) based on the analysis of flow logs. As UBI (Ultrasonic Borehole Imager) logs were not carried out in the open hole section of the GPK2 well, the orientation of the flowing fractures have been best-estimated by BRGM based on past experience of the deep-seated structures of the Soultz granite and on hydraulic data.

In the GPK3 well, UBI imaging along the entire granite section was performed. Relevant fracture parameters (depth, orientation, apparent aperture) have been also interpreted by BRGM. Along the open-hole sections, only the large and open fractures have been taken into account in the model. A

preliminary data set of these fractures, listed in the following table, was established from apparently relevant fracture thickness with clear response on the transit time at UBI images.

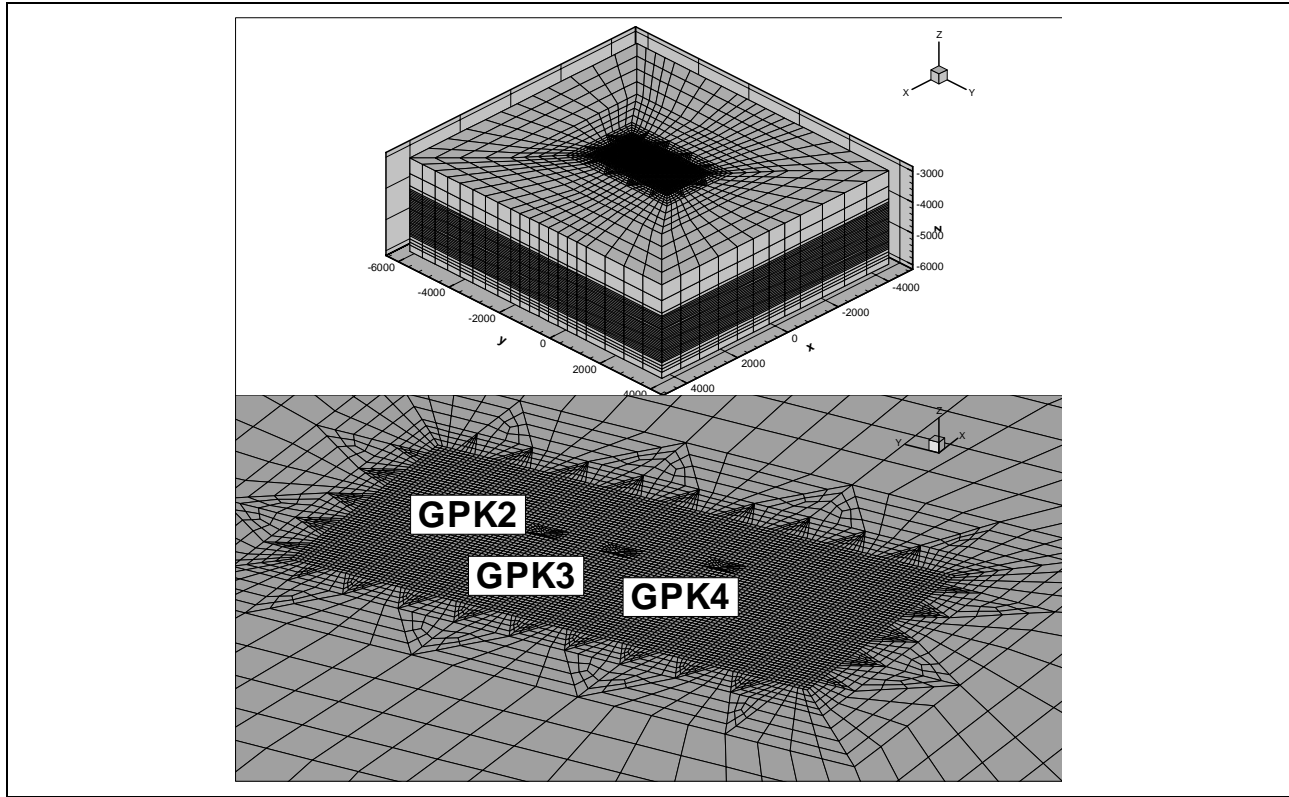


Fig. 6: FE model for the reservoir domain in Soultz-sous-Forêts with the 5 km boreholes GPK 2/3/4, used for the hydraulic calculations in HEX-S. Consisting of ~400'000 elements. North direction is aligned along the y-axis.

Table 1: Preliminary fracture data from GPK2 and GPK3

| Bore-hole | x | y | z | azimuth dip angle |
|-----------|--------|--------|---------|----------------------|
| GPK2 | 33.5 | -438.7 | -4394.8 | 250/70 |
| GPK2 | 11.8 | -419.5 | -4458.5 | 70/70 |
| GPK2 | -6.4 | -408.4 | -4525.1 | 70/70 |
| GPK2 | -53.7 | -376.6 | -4716.8 | 250/65 |
| GPK2 | -79 | -355.9 | -4816.5 | 250/65 |
| GPK2 | -108.5 | -337.8 | -4936.6 | 250/70 |
| GPK3 | 111.5 | -956.8 | -4517.4 | 122/66 |
| GPK3 | 111.5 | -956.8 | -4517.7 | 124/61 |
| GPK3 | 111.5 | -957.1 | -4542.3 | 330/54 |
| GPK3 | 111.5 | -957.1 | -4542.6 | 320/54 |
| GPK3 | 111.4 | -957.3 | -4569.1 | 307/60 |
| GPK3 | 111.7 | -960.4 | -4660.0 | 266/52 |
| GPK3 | 112.2 | -962.3 | -4685.9 | 065/68 |
| GPK3 | 112.3 | -962.7 | -4691.7 | 247/67 |
| GPK3 | 112.3 | -968.2 | -4992.8 | 249/40 |
| GPK3 | 111.8 | -966.7 | -4943.0 | 292/58 |
| GPK3 | 111.2 | -966.7 | -4971.3 | 356/48 |

In future calculations, a meanwhile slightly revised selection of the GPK3 fracture dataset has to be accounted for. Apart from the deterministic fractures intersecting the boreholes, deterministic fault zones at larger distance - derived from the location of microseismic events - and a stochastic fracture distribution in the intermediate rock matrix - calculated from the fracture distribution statistics - will be included in the model.

MODEL RESULTS

Hydraulic stimulation at GPK3 started on May 27th, 2003 at 12:50. This time represents the time "zero" for all our considerations. Although the total injection period extended to June 7th, the treated time span only covers 530'000 s (>6 days). Flow rate was varied in numerous steps, starting with 30 l/s at the first day. In a first phase, flow was stepwise reduced to 20 l/s until 170'000 s, then reestablished at 30 l/s until 280'000s and finally set to 50 l/s, with a short-time (~3 hr) high injection rate of 70 l/s. Due to misplaced pressure sensors, the downhole pressure

records had to be corrected using the borehole simulator HEX-B (Mégel 2005). Pressure response was less pronounced with a first pressure level at $\Delta P = 10$ MPa that nearly continuously increased until $\Delta P = 16$ MPa at $t = 530'000$ s, irrespective of decreasing flow rate at early stage. The complete flow rate and (corrected) pressure record can be recognized on Fig. 7.

The hydraulic simulation results do not fully reflect the described smooth ΔP -behavior. However, the base level and short-term pressure variation are generally well reproduced. Especially, if positive flow steps are well represented (note pressure variation at $t \approx 60'000$ s, $170'000$ s; and $290'000$ s). However, the effect of decreasing flow at the first stage is overestimated. A possible explanation is that the shearing aperture has been treated as irreversible and that the real transmissivity drops stronger at decreasing flow than anticipated by the model. Another impact might arise from the choice of the boundary condition. Very probably, the boundaries are less permeable than assumed – this effect could be strongly responsible for the continuous increase in

pressure. However, the strong non-linear behavior is especially well described. The flow regime is clearly non-linear, the increase of flow rate by 70% (29 to 50 l/s) only results in a 30% pressure increase, an effect that is very well explained by the data simulation. Another most important effect is the over-all little increase of reservoir transmissivity (or injectivity). Normalizing the pressure/flow record at an arbitrary 100% level at the end of the first flow step at injection, our model predicts a variation of relative injectivity that finally reaches 125% at $t \approx 530'000$ s. Although, the data indicated only 101% at the same time, the agreement is amazing, accounting for the strong cubic law between aperture change and permeability. Easily, the simulation could result in completely different orders of magnitude! Noteworthy is the effect of anisotropic flow elucidated by further sensitivity investigations. Flow seems to spread first in radial direction around the borehole, aligns however quickly in the direction of the flow field. This could cause a strong lateral pressure variation in the matrix, an effect that is also well known from the analysis of seismic locations.

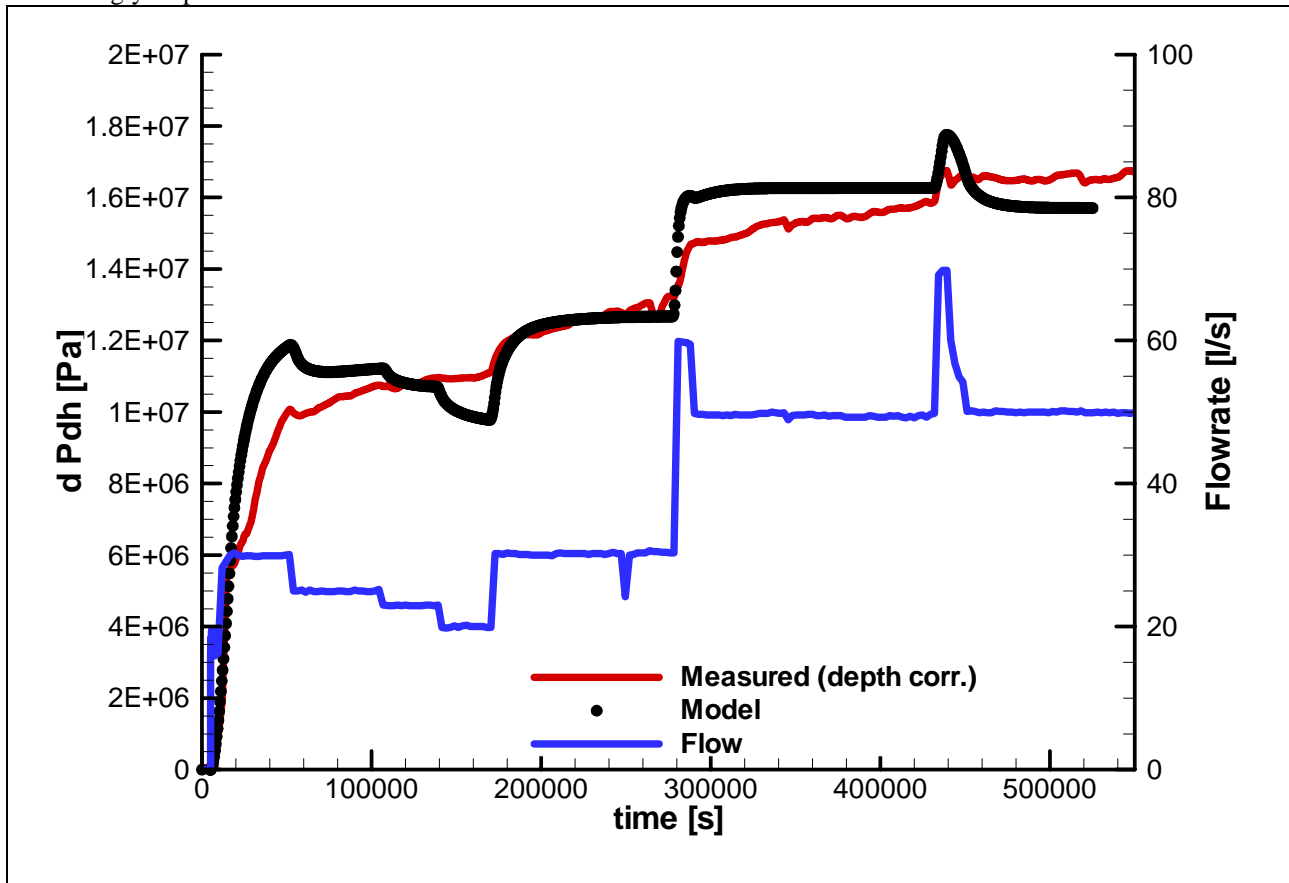


Fig. 7: Hydraulic data from stimulation of GPK3 starting 27. May 2003, 12:50. Pressure data are provided as differential pressure (compared to ambient situation) by a red line, quantified by the left axis; flow rate (blue line) is given at the right axis. Also provided are the modelled differential pressure data (frequent black dots).

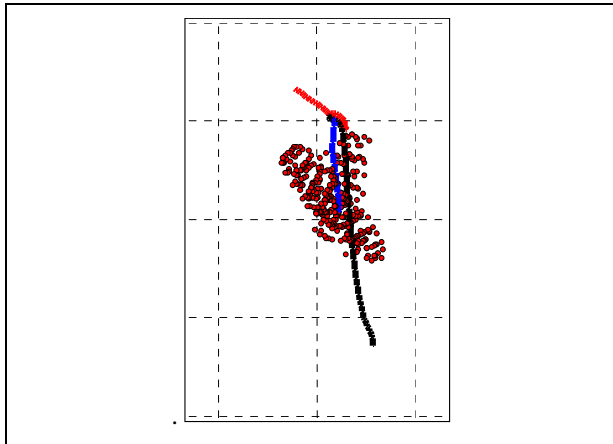


Fig. 8: Simulated shear failure (right). The plane view also illustrates the trajectories of the three boreholes (Red GPK2, blue GPK3 and black GPK4). The seismic cloud is spreading next to the injection at GPK3. The underlying grid has 500 m spacing.

Seismicity was strongly evolving starting next to GPK3. Already after the 1 day, the seismic cloud was spreading to distance of >500 m from open-hole (see also Asanuma 2004 for details). The general pattern of seismicity is directed in ~N-S direction, in agreement with the direction of the maximum horizontal stress direction, σ_{max} . As contribution to the determination of the stress field, it can be stated that our model clearly favour a pure normal stress field, a transfer into a strike-slip regime would cause unstable fracture system, right from the beginning of the simulation. The induced shearing events as simulated by HEX-S (under pure normal stress regime), also tends to spread in N-S direction. Since HEX-S simulates shear slippages when the shear stiffness is exceeded by the shear stress during a time step at optimum oriented fractures, also minimum slip displacement are simulated that certainly don't have any seismic significance (under the M -1 threshold). For a minimum slippage displacement of 0.5 cm, the simulated area is well in agreement with the located events. A different slippage threshold would not produce a strongly different pattern. Hence, it can be stated that HEX-S is well able to reproduce spatial constants of shear events that are identical to the extension of microseismic cloud. This, again, is a clear indication that the simulated pressure field in the rock matrix is well understood.

CONCLUSION

The new hydromechanical reservoir model HEX-S has been successfully tested on data from the European EGS site Soultz-sous-Forêts (France). The

model allows an insight in the complex reservoir behavior under the conditions of massive flow injections that are required for reservoir stimulation. HEX-S supplies a physical reservoir model by jointly interpreting the hydraulic field and the hydraulic-induced shearing events. A further important aspect is that the simulation of the dynamic reservoir behavior is strongly based on a combined data analysis integrating lithological, hydraulic, thermal and stress evaluation, such as evaluated in an excellent way at the Soultz project.

This also provides perspectives for future developments such as design calculations that enable optimizing cost-intensive hydraulic stimulations before hand under financial or logistical restrictions. Therewith it is also possible design optimum reservoir creation strategies or to quantify effects like dual-injections as proposed by Baria et al. (2004) under the conditions of Soultz-sous-Forêts, together with the seismic impact. Clearly, the prognosis of microseismicity is certainly a key factor for actual projects in Europe that are partly located in strongly populated areas.

REFERENCES

- Asanuma, H., T. Izumi, Y. Kumano, N. Soma, H. Niitsuma, R. Baria, and S. Michelet, 2003, Data Acquisition and Analysis of Microseismicity from the Stimulation at Soultz in 2003 by Tohoku University and AIST, Japan., *Geothermal Resource Council, 2004*, Palm Spring Sep. 2004
- Baria, R., Baumgärtner, J., Gérard, A., Garnish, J., 2000, The European HDR programme: main targets and results of the deepening of the well GPK2 to 5000 m. *In: Proc. World Geothermal Congress 2000*, p. 3643-3652.
- Baria R., Michelet S., J.Baumgaertner, B.Dyer, A.Gerard, J.Nicholls, T.Hettkamp, D.Teza, N.Soma, H.Asanuma, J. Garnish, T.Megel, 2004, Microseismic monitoring of the world's largest potential HDR reservoir, *Proc. Twenty-Ninth Workshop on Geothermal Reservoir Engineering Stanford University, Stanford, California, January 26-28, 2004*
- Bächler D., Evans K., Hopkirk R., Kohl T., Mégel T., Rybach L., Data Analysis and controls towards understanding reservoir behaviour and the creation of a conceptual model, Final Report to the Bundesamt für Bildung und Wissenschaft, Projekt 98.0008-1 - EU Project No. JOR3-CT98-0313, Bern, Switzerland
- Cuenot N., Dorbath C., Dorbath, L., 2005, Analysis of the microseismicity induced by fluid injections at the Hot Dry Rock site of Soultz-sous-Forêts (Alsace,

France): implications for the characterization of the geothermal reservoir properties, *Pure and Applied Geophysics*, submitted

Gérard A., 2004, Stimulation hydraulique du puit GPK3 et tests de circulation entre les puits GPK3 et GPK2 - Note de synthèse, *Rapport ADEME / GEIE "Exploitation Minière de la Chaleur No. 01.05.030"*

Kohl, T. and Hopkirk, R.J., 1995. "FRACTure" a simulation code for forced fluid flow and transport in fractured porous rock. *Geothermics*, 24(3): 345-359.

Evans K.F., Moriya H., Niitsuma H., Jones R. H., Phillips W. S., Genter A., Sausse J., Jung R., Baria R., 2005, Microseismicity and permeability enhancement of hydrogeologic structures during massive fluid injections into granite at 3 km depth at the Soultz HDR site, *Geophys. J. Int.*, 160: 388-412.

Jing, Z., Watanabe, K., Willis-Richards, J. and Hashida, T., 2002. A 3-D water/rock chemical interaction model for prediction of HDR/HWR geothermal reservoir performance. *Geothermics*, 31: 1-28.

Maurer R., 2004, Erstellung von Kluftmodellen und vergleichende hydraulische Modelle des geothermischen Reservoirs von Soultz-sous-Forêts, *Diploma Thesis Univ. Freiburg (D)*, 95 p

Mégel, T., Kohl, T., Gérard, A., Rybach, L., Hopkirk, R., 2005, Downhole pressures derived from wellhead measurements during hydraulic experiments, *Proceedings World Geothermal Congress 2005, Antalya, Turkey*

Willis-Richards, J., Watanabe, K. and Takahashi, H., 1996. Progress toward a stochastic rock mechanics model of engineered geothermal systems. *Journal of Geophysical Research*, 101(B8): 17,481-17,496.

ACKNOWLEDGEMENTS

The authors are very grateful to the Swiss Federal Office of Education and Science and to the Swiss Federal Office for Energy which support (under the contract number 03.0460) this research, under the EU contract (SES6-CT-2003-502706). Also the support from EEIG staff in Soultz-sous-Forêts, their subcontractors and especially Dimitra Teza is thankfully acknowledged.

The authors want to acknowledge especially R. Maurer's involvement, providing geological data and performing HEX-S sensitivity analyses during his diploma thesis. Especially, the authors express their appreciation to C. Dezayes and A. Genter from the BRGM (French Geological Survey) who deliberately provided their data.